

Ascorbic Acid Induced Enhancement of Room Temperature Phosphorescence of Sodium Tripolyphosphate-Capped Mn-Doped ZnS Quantum Dots: Mechanism and Bioprobe Applications

He-Fang Wang, Yan Li, Ye-Yu Wu, Yu He, and Xiu-Ping Yan*^[a]

Abstract: Although quantum dot (QD)-based room temperature phosphorescence (RTP) probes are promising for practical applications in complex matrixes such as environmental, food and biological samples, current QD-based-RTP probes are not only quite limited but also exclusively based on the RTP quenching mechanism. Here we report an ascorbic acid (AA) induced phosphorescence enhancement of sodium tripolyphosphate-capped Mn-doped ZnS QDs, and its application for turn-on RTP detection. The chelating ability allows AA to extract the Mn and Zn from the surface of the

QDs and to generate more holes which are subsequently trapped by Mn^{2+} , while the reducing property permits AA to reduce Mn^{3+} to Mn^{2+} in the excited state, thereby enhancing the excitation and orange emission of the QDs. The enhanced RTP intensity of the QDs increases linearly with the concentration of AA in the range of 0.05–0.8 μM . Thus, a QD-based RTP probe for AA is developed. The proposed

QD-based turn-on RTP probe avoids tedious sample pretreatment, and offers good sensitivity and selectivity for AA in the presence of the main relevant metal ions and other molecules in biological fluids. The limit of detection (3 σ) of the developed method is 9 nM AA, and the relative standard deviation is 4.8% for 11 replicate detections of 0.1 μM AA. The developed method is successfully applied to the analysis of real samples of human urine and plasma for AA with quantitative recoveries from 96 to 105%.

Keywords: ascorbic acid • phosphorescence • quantum dots • sensors • sodium tripolyphosphate

Introduction

The unique properties of quantum dots (QDs), such as composition- and size-dependent emission wavelength, broad and intense absorption band, narrow and symmetric emission profile, and good resistance to photobleaching, have attracted considerable interest in diverse fields.^[1–3] QD-based optosensing is one of the widely explored fields owing to the abstruse surface chemistry of functionalized QDs. To date, QD-based fluorescent sensors have been studied much more extensively than QD-based phosphorescent sensors owing to the more usual phenomenon of QD-based fluorescence over phosphorescence.^[4] However, phosphorescence provides several important advantages over fluorescence, such as

long emission lifetime, wide gap between excitation and emission spectra, and minimal interference from short-lived autofluorescence and scattering light.^[4,5] Consequently, QD-based room temperature phosphorescence (RTP) sensors are promising for practical applications in complex matrixes such as environmental, food and biological samples.

Recently, RTP of QDs has received increasing attention for optosensing applications.^[4b,6] Owing to the long RTP lifetime, any scattering light and the autofluorescence of the complex matrix can be effectively avoided.^[6] Thus, the QD-based-RTP probes can detect the targets in biological fluids and environmental water without the need for tedious sample pretreatment.^[6] However, previous QD-based-RTP probes are exclusively based on the RTP quenching mechanism, and such signal-quenching probes suffer from high background, which usually results in higher limits of detection (LODs). In contrast, the turn-on probes can have lower background, therefore of novel QD-based enhanced RTP probes is therefore of great significance for improving the detection capability.^[7]

Ascorbic acid (AA) is an essential nutritional factor, participating in many life processes as an important enzyme co-

[a] H.-F. Wang, Y. Li, Y.-Y. Wu, Y. He, X.-P. Yan
Research Center for Analytical Sciences
College of Chemistry, Nankai University
94 Weijin Road, Tianjin 300071 (China)
Fax: (+86) 22-23506075
E-mail: xpyan@nankai.edu.cn

Supporting information for this article is available on the WWW under <http://dx.doi.org/10.1002/chem.201001093>.

factor and antioxidant.^[8a] The reported strategy for AA detection has spanned electrochemical,^[8] spectrophotometric,^[9] as well as chromatographic^[10] methods. Among them, fluorescent probes/sensors possess the merits of higher sensitivity and convenience. Recently, several optosensors for detecting AA have been reported, such as a microplate calorimetric biosensor with a LOD of 0.8 nM,^[11] a water-soluble off-on spin-labeled QD conjugate based sensor with a LOD of 4.33 μM ,^[12] and a QD-based off-on fluorescent probe modulated by a simple chemical oxidation with a LOD of 74 nM.^[13]

Herein, we report a novel AA induced RTP enhancement system based on sodium tripolyphosphate capped Mn-doped ZnS (STPP-ZnS-Mn) QDs. To the best of our knowledge, this is the first report of the QD-based RTP turn-on system. We employed various techniques, such as photofluorometry, inductively coupled plasma mass spectrometry (ICP-MS), and cyclic voltammetry to gain an insight into the mechanism of the AA-induced RTP enhancement of STPP-ZnS-Mn QDs. We also explored the STPP-ZnS-Mn QD-based turn-on RTP system for rapid, cost-effective, and selective detection of AA in biological fluids.

Results and Discussion

Preparation and characterization of STPP-ZnS-Mn QDs:

Both thiols (e.g., mercaptopropionic acid,^[6c,d,14] L-cysteine,^[6a] and cysteamine,^[15]) and non-thiols (e.g., polyphosphates^[16,17a]) have been employed to synthesize water-soluble Mn-doped ZnS QDs. Compared with thiols, which are readily oxidized and have strong affinity to the metals in QDs, polyphosphates are not only difficult to oxidize, but also show weak affinity to the metals in QDs, thereby leaving more chance for the analytes to interact with QDs. So, in this work we also used a non-thiol, STPP, as the ligand to synthesize the STPP-ZnS-Mn QDs, as was reported by Warad et al.^[16] All steps of the synthesis were carried out in water at room temperature or in an ice bath without the need for a protective atmosphere. Compared with a previous procedure for the preparation of STPP-ZnS-Mn QDs,^[16] room temperature agitation of the mixture of the ligand and the acetates used in this work rather than heating to reflux resulted in convenient operation.

The high resolution transmission electron microscopy (HRTEM) image shows that the prepared spherical STPP-ZnS-Mn QDs have almost uniform size with a diameter of 4.2 ± 0.4 nm (Figure 1a), in agreement with the estimation obtained by using the Debye-Scherrer equation from the XRD pattern (Figure 1b). Similar to other Mn-doped ZnS QDs, the STPP-ZnS-Mn QDs also exhibit a cubic structure (or zinc-blende) with peaks for (111), (220), and (311) planes of ZnS (Figure 1b). The FTIR spectra of STPP-ZnS-Mn QDs also show the characteristic peak of the Zn-S vibration band at 1101 cm^{-1} (Figure 1c).^[18] ICP-MS analysis reveals that the prepared STPP-ZnS-Mn QDs contain 0.061% Mn, 20.3% Zn, and 2.7% P. Owing to the small

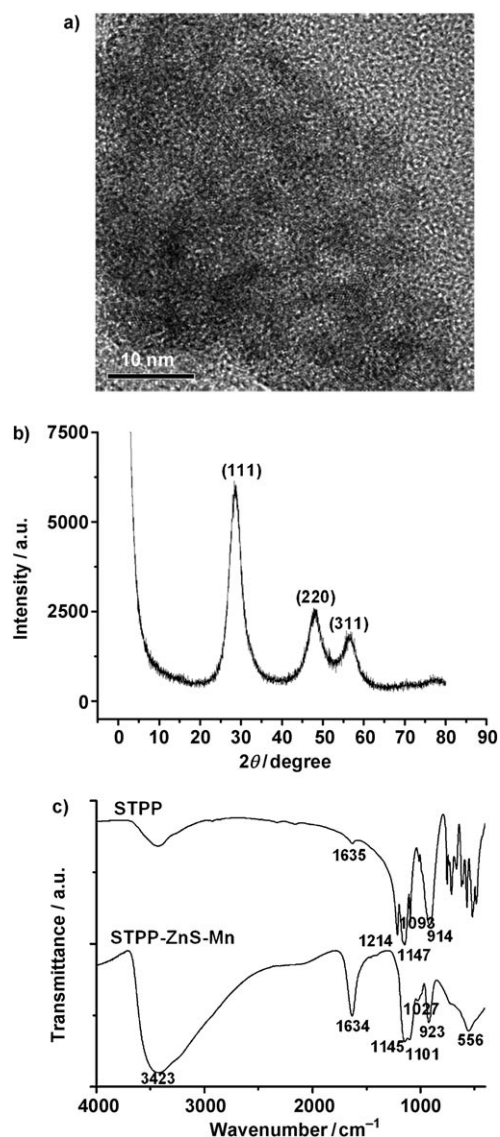


Figure 1. a) HRTEM image of the prepared STPP-ZnS-Mn QDs; b) XRD pattern of the prepared STPP-ZnS-Mn QDs; c) FTIR spectra of STPP and the prepared STPP-ZnS-Mn QDs.

amount of STPP in the QDs, no obvious bands at 1214, 1147, or 1093 cm^{-1} (stretching vibration of PO_3) of STPP was observed in the FTIR spectra of the QDs. The peaks of 1634 and 923 cm^{-1} mostly arise from the residual humidity in the sample during sample preparation as their intensity decreased after the QDs and KBr were further dried at 100°C in vacuum (Figure S1 in the Supporting Information). The absolute quantum yield of STPP-ZnS-Mn QDs was 17.9%.

AA-induced RTP enhancement of STPP-ZnS-Mn QDs:

Figure 2 shows the dependence of the RTP emission spectra of 2 mg L^{-1} STPP-ZnS-Mn QDs on the concentration of AA buffered with 10 mM tris(hydroxymethyl) aminomethane (Tris)-HCl (pH 7.4). Addition of AA significantly enhances

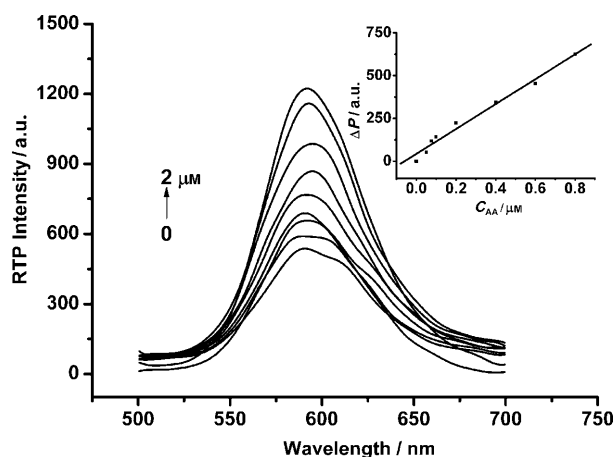


Figure 2. Dependence of the RTP emission spectra of 2 mg L^{-1} STPP-ZnS-Mn QDs under excitation at 316 nm on the concentration of AA buffered with 10 mM Tris-HCl (pH 7.4). Inset shows the enhanced RTP intensity of 2 mg L^{-1} STPP-ZnS-Mn QDs vs. the concentration of AA.

the RTP intensity of STPP-ZnS-Mn QDs. Moreover, the AA-induced enhancement of the RTP of STPP-ZnS-Mn QDs is both AA concentration (Figure 2) and pH dependent (line b, Figure 3). The enhanced RTP intensity (ΔP) remains unchanged from weak acidic (pH 6.5) to physiological

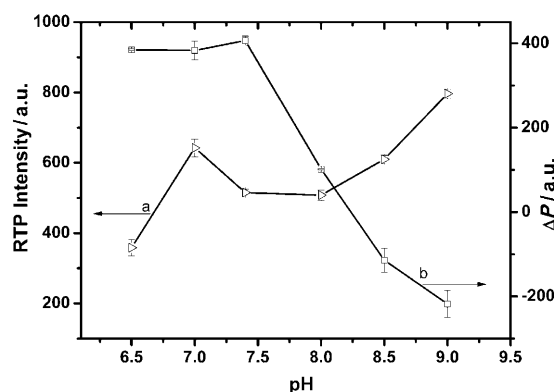


Figure 3. pH-Dependent RTP intensity of 2 mg L^{-1} STPP-ZnS-Mn QDs in the absence of AA, and the enhanced RTP intensity upon the addition of 0.5 μM AA.

condition (pH 7.4), but rapidly decreases in the pH range of 8.0–9.0. There are two aspects associated with such a pH effect. On one hand, the surface state of the STPP-ZnS-Mn QDs is significantly pH-dependent (line a, Figure 3). On the other hand, the pH value also has a great influence on the speciation of AA: AA ($pK_a = 4.2$) at pH 6.5–7.4 exists as the resonance structure ascorbate form, which increases its chelating capability with metals; whereas in basic media AA is easily oxidized and decomposed,^[19a] which could be the reason for the rapid decrease of ΔP under basic conditions. Considering the biological activity of AA, the physiological condition (pH 7.4) was chosen for AA detection.

To evaluate the sensitivity of the STPP-ZnS-Mn QDs for the RTP detection of AA, the RTP intensity of STPP-ZnS-Mn QDs at 595 nm was monitored as a function of C_{AA} (inset of Figure 2). There is a linear relationship between ΔP and C_{AA} ($\Delta P = 42.7 + 727.1 C_{AA}$, C_{AA} in μM) in the range of 0.05–0.8 μM with a correlation coefficient of 0.9913. Moreover, no change of the relationship between the enhanced RTP intensity and C_{AA} was observed even after removal of the dissolved free oxygen in the aqueous solution of STPP-ZnS-Mn QDs by inert gas purging. The LOD of the developed RTP probe, which was calculated as the concentration of AA equivalent to three times the standard deviation for eleven replicate detections of ΔP at 0.05 μM AA, was 9 nM, whereas the relative standard deviation for eleven replicate detections of 0.1 μM AA was 4.8%. Since the dynamic range is narrow similar to other QD-based probes,^[6a,b,13] an appropriate dilution is required for real sample analysis.

RTP response of STPP-ZnS-Mn QDs to AA-related compounds:

Since the chemical and biological functions of AA are related to the two adjacent hydroxyl groups linked to the C=C bond, we also suppose that those groups might also be responsible for the AA-induced RTP enhancement. So, we first evaluated the RTP response of STPP-ZnS-Mn to AA-related compounds, including the redox-related and degradation products of AA (L-dehydroascorbic acid (DAA), 2,3-diketo-L-gulonic acid (DKG), L-gluconic acid γ -lactone (GAL), xylose, and oxalic acid), and diphenols (dopamine, catechol, resorcin and quinol). Figure 4 shows the different RTP responses of STPP-ZnS-Mn QDs to the selected compounds.

Although DAA, DKG, GAL, and xylose also contain adjacent hydroxyl groups, they induce much less enhancement of the RTP response of STPP-ZnS-Mn QDs than AA (Figure 4). Such different RTP responses may arise from the different properties (such as acidity, reducing and chelating properties with metals) of the OH groups, which are connected to the C–C bond in DAA, DKG, GAL, and xylose, as opposed to the C=C bond in AA.

Oxalic acid, however, leads to the RTP quenching of STPP-ZnS-Mn QDs. Although oxalic acid also contains hydroxyl groups, the OH groups link up with a carbonyl group, which is not the case for AA in which the OH groups link up with a C=C bond. The RTP quenching of STPP-ZnS-Mn QDs by oxalic acid is in agreement with the pH-dependent RTP response of AA at pH 8.0–9.0 (line b, Figure 3) because AA is most likely to degrade into oxalic acid under basic conditions.^[19a]

Dopamine and catechol, with the two adjacent hydroxyl groups linked to a C=C bond as in AA, also enhance the RTP emission of STPP-ZnS-Mn QDs, but to a much lesser extent than AA. However, the induced ΔP signal by resorcin and quinol is negligible owing to the quite different space position of the hydroxyl groups (1,3- or 1,4-). The relatively small ΔP induced by dopamine and catechol can be ascribed to the less favorable interactions resulting from the neutral form of dopamine and catechol ($pK_a \approx 9.5$) at the

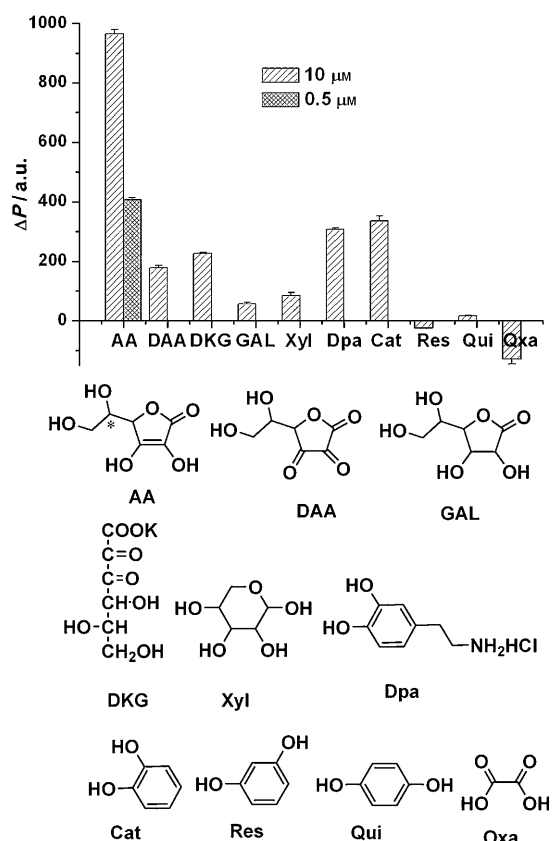


Figure 4. Enhanced RTP response of the 2 mg L^{-1} STPP-ZnS-Mn by AA ($10 \mu\text{M}$ and $0.5 \mu\text{M}$) and other structurally related compounds: L-dehydroascorbic acid (DAA), 2,3-diketo-L-gulonic acid (DKG), L-gluconic acid γ -lactone (GAL), xylose (Xyl), dopamine (Dpa), catechol (Cat), resorcin (Res), quinol (Qui), and oxalic acid (Oxa) (all $10 \mu\text{M}$).

working pH of 7.4, as well as the electronic delocalization of the aromatic benzene, which decreases the negative charges of the O atoms.

The above-mentioned results indicate that the two adjacent hydroxyl groups linked to the C=C bond of AA (in ascorbate form at $\text{pH} > 4.2$) are the most probable sites responsible for RTP enhancement. This is further ascertained by the similar RTP enhancement of L- and D-AA (Figure S2 in the Supporting Information), since L- and D-AA have the same structure except the spatial arrangement of the hydroxyl group linked to the asymmetric carbon atom (*; Figure 4).

Possible mechanisms for the AA-induced RTP enhancement of STPP-ZnS-Mn QDs: AA is an important biological molecule with many biological functions, such as the essential nutritional factor, the antioxidant and the enzyme cofactor. These significant roles of AA are related to the two adjacent hydroxyl groups linked to the C=C bond, the redox property of which makes AA a well-known antioxidant and the chelating ability with metals makes AA an important enzyme cofactor. The above results and the following experiments also show that the redox and chelating properties

of the two adjacent hydroxyl groups linked to the C=C bond of AA would be the reasons for the RTP enhancement of the QDs.

The most probable sites for STPP-ZnS-Mn QDs to interact with AA are through Zn or Mn at the surface of the QDs. The electron-rich ascorbate form of AA is negatively charged at the working pH of 7.4, so it is not possible for AA to interact with the ligand STPP, which is also negatively charged at the working pH. To elucidate these points, we performed dialysis experiments to evaluate the concentration of Mn, Zn, and P in the solution of the STPP-ZnS-Mn QDs in the absence and presence of AA (Table S1 in the Supporting Information). Mn, Zn, and P were detected in the dialysate of QDs due to the dynamic dissolution/crystallization equilibrium. The chelation of AA (in the form of ascorbate at working pH) with the metals makes that equilibrium shift towards dissolution, resulting in a significant increase in the concentration of Mn and Zn in the dialysate in the presence of AA. However, the concentration of STPP (revealed by P) in the dialysate of QDs in the absence and presence of AA does not vary significantly, indicating that addition of AA does not result in the significant flaking of the STPP ligands off the QDs. Moreover, the concentration of STPP in the dialysate of QDs is high (about 80% of the total STPP attached onto the QDs), indicating the weak binding of the ligand STPP onto the QDs. The weaker binding of the ligand gives more chance for AA to interact with metals of STPP-ZnS-Mn QDs, resulting in higher sensitivity to AA than thiol-capped ZnS-Mn QDs. The observed decrease in the contents of Zn (about 1.9% of total Zn) and Mn (about 2% of total Mn) in the STPP-ZnS-Mn QDs, and the decrease of the particle size of the STPP-ZnS-Mn QDs in the presence of AA after dialysis (Figure S3 in the Supporting Information) supports that AA extracts the metals from the surface of the STPP-ZnS-Mn QDs.

The chelating ability and reducing property of AA are responsible for the enhanced excitation efficiency of STPP-ZnS-Mn QDs (Figure S4 in the Supporting Information). The excitation of the Mn-doped ZnS QDs starts with the creation of the electron-hole pair,^[17] so any factors favorable for the formation of electron-hole pairs can enhance the excitation efficiency. As shown above, AA extracts some metals from the surface of STPP-ZnS-Mn QDs, thereby generating more holes which are trapped by Mn^{2+} [Eq. (1)]. On the other hand, the electron-rich ascorbate form of AA could result in electrons recombining with Mn^{3+} [Eq. (2)], resulting in Mn^{2+} in an excited state. This process is confirmed by the cyclic voltammetry of the bare glassy carbon electrode (GCE), GCE modified with STPP-ZnS-Mn QDs in the absence and presence of AA (Figure 5). The reduction peak around -1.5 V of the GCE modified with STPP-ZnS-Mn QDs disappeared in the presence of AA, indicating the reduction of Mn^{3+} to $(\text{Mn}^{2+})^*$ by AA.^[20] As AA promotes the generation of the Mn^{2+} excited state, the following well-known orange emission of Mn^{2+} (${}^4\text{T}_1\text{-}{}^6\text{A}_1$) is enhanced [Eq. (3)].

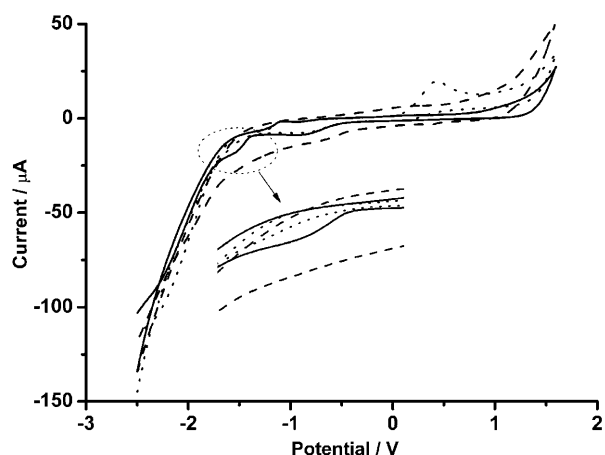


Figure 5. The cyclic voltammograms of bare GCE (----), GCE modified with STPP-ZnS-Mn QDs in the absence (—) and presence (.....) of 2 mM AA at 10 mM pH 7.4 Tris-HCl. The potential scanned in the positive direction from -2.5 to $+1.6$ V with a scan rate of 100 mVs^{-1} .



To ascertain whether AA has any effect on ZnS defect-related emission, the photoluminescent spectra of STPP-ZnS-Mn QDs in the absence and presence of AA are compared (Figure 6). Mn-doped ZnS QDs have two photoluminescent emissions, the blue one at about 425 nm and the orange one at about 595 nm. The former is short-lived and can not be observed in phosphorescence mode, whereas the latter appears in RTP spectra owing to its long lifetime. The photoluminescent spectra of STPP-ZnS-Mn QDs were obtained under excitation at 330 nm instead of 316 nm to avoid the

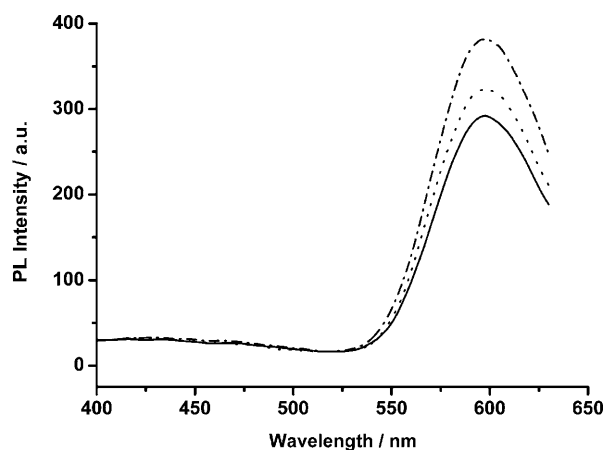


Figure 6. The photoluminescent spectra of 2 mg L^{-1} STPP-ZnS-Mn QDs before and after addition of AA buffered by 10 mM pH 7.4 Tris-HCl. The PL spectra were obtained under excitation at 330 nm. The slit of excitation and emission are both set at 10 nm and the PMT voltage is -700 V. STPP-Zn-Mn (—), STPP-Zn-Mn + $0.5 \mu\text{M}$ AA (.....), STPP-Zn-Mn + $10 \mu\text{M}$ AA (-.-.-).

overlap of the double-wavelength peak of the excitation. Figure 6 shows that the weak blue emission of the STPP-ZnS-Mn QDs at 425 nm is much less sensitive than the orange emission at 595 nm upon the addition of AA, excluding the possibility of defect-related interaction of AA and STPP-ZnS-Mn QDs.

The presence of AA also significantly increases the RTP lifetime of the STPP-ZnS-Mn QDs (Table S2 in the Supporting Information), as revealed by the evident changes of the decay curves of the orange emission at 595 nm (excited by N_2 laser at 337 nm, Figure 7). These results indicate that

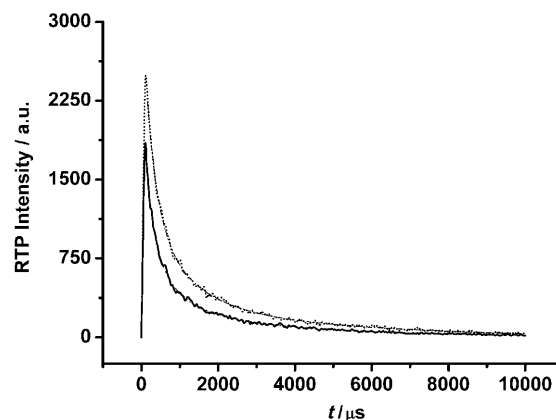


Figure 7. The decay curves of the RTP emission of 10 mg L^{-1} STPP-ZnS-Mn QDs before and after addition of $10 \mu\text{M}$ AA buffered by 10 mM pH 7.4 Tris-HCl. The three averaged scans of RTP emission at 595 nm (300 channels) were recorded by the excitation of a N_2 laser at 337 nm. The emission slit was set at 10 nm. STPP-Zn-Mn (—), STPP-Zn-Mn fitting (----), STPP-Zn-Mn + AA (.....), STPP-Zn-Mn + AA fitting (-.-.-).

the addition of AA results in either an increase of the Mn^{2+} emission or a reduction of nonradiative decay of STPP-ZnS-Mn QDs. The luminescence efficiency (h) can be expressed as $h = (1 + D^2\tau_R/\tau_{NR})^{-1}$, in which τ_R and τ_{NR} are the radiative and nonradiative decay time and D is the volume of a nanoparticle.^[21,22] As the particle size diminishes (Figure S3 in the Supporting Information), the D^2 should decrease a lot, despite the increase of τ_R (Table S2 in the Supporting Information) and decrease of τ_{NR} , the h increases. According to the above mechanism, the STPP-ZnS-Mn QDs based RTP probe is not reusable because of the extraction of the metals from the QDs by AA, which, nevertheless, does not limit the applications of the QD-based RTP probe due to the easy fabrication and low consumption of the QDs.

Application of the STPP-ZnS-Mn QD-based RTP probe for detecting AA in biological fluids: To further evaluate the selectivity of the STPP-ZnS-Mn QD-based RTP probe for detecting AA, the effects of the main relevant metal ions and molecules in biological fluids, and some structurally related compounds were examined (Table S3 in the Supporting Information). The enhanced RTP due to the addition of $0.1 \mu\text{M}$ AA was unaffected by a 30000-fold excesses of Na^+ ,

15000-fold excesses of K^+ , 300-fold excesses of Mg^{2+} , and a 50-fold excesses of Ca^{2+} . Amino acids, like arginine and histidine, at a 10000-fold concentration of AA did not affect the detection of AA, but the co-existence of L-cysteine was only permitted at a 10-fold excess. Other structurally related compounds, such as DAA, DKG, and Dpa, at 50-times the concentration of AA did not affect the detection of AA. Reducing agents, such as glucose, GAL, xylose, citric acid, uric acid, and reduced nicotinamide adenine dinucleotide (NADH) were tolerable at 20000-, 35000-, 200-, 500-, 300-, and 200-fold concentration of AA, respectively.

The STPP-ZnS-Mn QD-based RTP probe was applied to the detection of AA in urine and plasma samples. It is reported that both the urine and plasma samples show significant autofluorescent background, but negligible RTP background.^[6a] The remarkable merits of the RTP makes it promising for the analysis of complex samples, such as biological fluids, avoiding tedious sample pretreatment procedures. To meet the linear range of the proposed STPP-ZnS-Mn QD-based RTP probe for AA detection, the urine and plasma samples were diluted 1000-fold, which also ensured minimum interference from some concomitants such as dopamine and L-cysteine in urine and plasma (owing to their lower concentrations and lower sensitivity). Table S4 (Supporting Information) shows the analytical results of the urine and plasma samples, with the recoveries of the spiked AA in the diluted biological fluids from 96 to 105%. The above results demonstrate the potential applicability of the STPP-ZnS-Mn QD-based RTP probe for the detection of AA in biological fluids.

Conclusion

We have reported the AA-induced RTP enhancement system based on STPP-ZnS-Mn QDs. The turn-on RTP response is related to the two adjacent hydroxyl groups linked to the C=C bond of AA. The chelating ability allows AA to extract the Mn and Zn from the surface of the QDs and to generate more holes that are subsequently trapped by Mn^{2+} , while the reducing property permits AA to reduce Mn^{3+} to Mn^{2+} in the excited state, thereby enhancing the excitation and orange emission of the QDs. This preliminary mechanism would help to develop other QD-based RTP turn-on systems. The STPP-ZnS-Mn QD-based turn-on RTP system shows good performance for AA detection without the need for tedious sample pretreatment.

Experimental Section

Materials and chemicals: All chemicals used were at least of analytical grade and were used without further purification. High purity water (18.2 M Ω cm) was obtained from a WaterPro water purification system (Labconco Co., Kansas City, U.S.A.). $Zn(CH_3COO)_2 \cdot 2H_2O$, $Mn(CH_3COO)_2 \cdot 4H_2O$, and $Na_2S \cdot 9H_2O$ were from Tianjin Kaitong Chemicals Co. (Tianjin, China), the Second Chemicals Co. of Shenyang (Shenyang, China), and Tianjin Sitong Chemicals Co. (Tianjin, China), respectively.

AA was purchased from the First Chemicals Co. of Tianjin (Tianjin, China) and D-AA was from Acros (Geel, Belgium). DAA and DKG were synthesized according to a literature procedure.^[19] GAL and NADH were from Aladdin (Shanghai, China) and Newprobe (Beijing, China), respectively. Tris, STPP, oxalic acid, xylose, dopamine hydrochloride, catechol, resorcin and quinol were obtained from Tianjin Guangfu Fine Chemical Research Institute (Tianjin, China). The Tris-HCl solution (0.1 M, pH 6.5–9.0) was used as the buffer solution.

Synthesis of STPP-ZnS-Mn QDs: The STPP-ZnS-Mn QDs were synthesized according to a literature procedure,^[16] but with modifications. Typically, all steps of the synthesis were carried out in water at room temperature or in an ice bath. In a 100 mL flask, $Zn(CH_3COO)_2$ (125 mmol) was dissolved in high purity water (30 mL), to which STPP (250 mmol) and $Mn(CH_3COO)_2$ (5 mmol) were added. After the mixture was stirred at room temperature for 30 min, Na_2S aqueous solution (10 mL, 12.5 M) was added dropwise and kept stirring in an ice bath for 10 min. Then, the mixture was stirred at room temperature for 2 h. Finally, the resultant STPP-ZnS-Mn QDs were centrifuged, washed with high purity water and absolute ethanol three times, and dried in a vacuum.

Instrumentation: FTIR spectra (4000–400 cm^{-1}) in KBr were recorded on a Magna-560 spectrometer (Nicolet, Madison, WI). The XRD spectra were collected on a Rigaku D/max-2500 X-ray diffractometer with $Cu_{K\alpha}$ radiation (Rigaku, Japan). The morphology and microstructure of STPP-ZnS-Mn QDs were characterized by HRTEM on a Philips Tecnai G2 F20 microscope (Philips, Holland). The samples for HRTEM were obtained by drying sample droplets from a dispersion in water onto a 300-mesh Cu grid coated with a lacy carbon film. The decayed curves of RTP emission at 595 nm excited by the N_2 laser at 337 nm were recorded on a PTI QM/TM/NIR system (Birmingham, NJ). The absolute quantum yield was measured on a FLS920 spectrometer (Edinburgh, UK). The cyclic voltammograms were monitored with a Model LK98BII microcomputer-based electrochemical analyzer (Tianjin Lanlike High-Tech Company, Tianjin, China). A traditional three-electrode system was employed with Pt wire as the counter electrode, Ag/AgCl/KCl as the reference electrode, and a 3 mm diameter GCE as the working electrode. The GCE was polished and ultrasonically cleaned in ethanol and water before use. The STPP-ZnS-Mn QD-modified GCE was prepared by dropping 5 μ L of 0.4 $mg L^{-1}$ of the QDs on the surface of the clean GCE and then dried in the dark at room temperature.

For the determination of the Mn, Zn, and STPP content in the solution of the QDs, STPP-ZnS-Mn QDs (320 $mg L^{-1}$, 5 mL) in the absence and presence of 2 mM AA were dialyzed by using a dialysis bag with a molecular weight cut-off of 12000–14000 (ShangHai DingGuo Biology, Shanghai, China) in 80 mL of 10 mM Tris-HCl buffer (pH 7.4), and the dialysate after acidification with 1% HNO_3 was analyzed on an X series ICP-MS instrument (Thermo Elemental, Cheshire, UK). For the determination of the Mn, Zn, and P in the solid QDs, STPP-ZnS-Mn QDs (1.6 mg) was dispersed in 80 mL of a 10×10^{-3} M Tris-HCl buffer (pH 7.4) and acidified with 1% HNO_3 before ICP-MS determination.

Phosphorescence measurement: The phosphorescence measurements were performed on an F-4500 spectrofluorometer (Hitachi, Japan) equipped with a plotter unit and a quartz cell (1 \times 1 cm). The excitation wavelength was 316 nm when the spectrofluorometer was set in the phosphorescence mode. The slit widths of excitation and emission were 10 nm and 20 nm, respectively. The PMT voltage was set at -950 V. An STPP-ZnS-Mn QDs suspension (400 $mg L^{-1}$) was prepared and stored under ambient conditions. The RTP signal of the QDs was stable for at least three months. A 10 mL mixture of 2 $mg L^{-1}$ STPP-ZnS-Mn, 10 mM Tris-HCl buffer and a given concentration of analyte standard solution were mixed thoroughly before RTP measurements.

Samples: The urine samples were collected from two healthy volunteers and the plasma samples were donated by a local hospital. An appropriate dilution of urine and plasma (1000-times) were adopted before detection. No further complex pretreatment and deproteinization procedures were needed for sample preparation.

Acknowledgements

This work was supported by the National Natural Science Foundation of China (grant nos.: 20977049 and 20935001), the National Basic Research Program of China (grant no.: 2006CB705703), and the Tianjin Natural Science Foundation (grants nos.: 09JCYBJC03900 and 10JCZDJC16300).

- [1] a) M. Bruchez, Jr., M. Moronne, P. Gin, S. Weiss, A. P. Alivisatos, *Science* **1998**, *281*, 2013–2016; b) W. C. W. Chan, S. M. Nie, *Science* **1998**, *281*, 2016–2018; c) S. Coe, W. K. Woo, M. Bawendi, V. Bulović, *Nature* **2002**, *420*, 800–803; d) E. M. Ali, Y. G. Zheng, H. H. Yu, J. Y. Ying, *Anal. Chem.* **2007**, *79*, 9452–9458; e) D. B. Cordes, S. Gamsey, B. Singaram, *Angew. Chem.* **2006**, *118*, 3913–3916; *Angew. Chem. Int. Ed.* **2006**, *45*, 3829–3832; f) Y. F. Chen, Z. Rosenzweig, *Anal. Chem.* **2002**, *74*, 5132–5138.
- [2] a) H. S. Jang, H. Yang, S. W. Kim, J. Y. Han, S. G. Lee, D. Y. Jeon, *Adv. Mater.* **2008**, *20*, 2696–2702; b) A. Rizzo, M. Mazzeo, M. Palumbo, G. Lerario, S. D'Amone, R. Cingolani, G. Gigli, *Adv. Mater.* **2008**, *20*, 1886–1891; c) W. U. Huynh, J. J. Dittmer, A. P. Alivisatos, *Science* **2002**, *295*, 2425–2427; d) P. Brown, P. V. Kamat, *J. Am. Chem. Soc.* **2008**, *130*, 8890–8891; e) S. Günes, H. Neugebauer, N. S. Sariciftci, J. Roither, M. Kovalenko, G. Pillwein, W. Heiss, *Adv. Funct. Mater.* **2006**, *16*, 1095–1099; f) R. Freeman, I. Willner, *Nano Lett.* **2009**, *9*, 322–326.
- [3] a) I. Robel, V. Subramanian, M. Kuno, P. V. Kamat, *J. Am. Chem. Soc.* **2006**, *128*, 2385–2393; b) R. J. Martín-Palma, M. J. Manso, V. Torres-Costa, *Sensors* **2009**, *9*, 5149–5172; c) I. L. Medintz, H. T. Uyeda, E. R. Goldman, H. Mattoussi, *Nat. Mater.* **2005**, *4*, 435–446; d) J. P. Yuan, W. W. Guo, E. K. Wang, *Anal. Chem.* **2008**, *80*, 1141–1145; e) W. J. Jin, M. T. Fernández-Argüelles, J. M. Costa-Fernández, R. Pereiro, A. Sanz-Medel, *Chem. Commun.* **2005**, 883–885; f) X. J. Wang, M. J. Ruedas-Rama, E. A. H. Hall, *Anal. Lett.* **2007**, *40*, 1497–1520.
- [4] a) J. Kuijt, F. Ariese, U. A. Th. Brinkman, C. Gooijer, *Anal. Chim. Acta* **2003**, *488*, 135–171; b) I. Sánchez-Barragán, J. M. Costa-Fernández, M. Valledor, J. C. Campo, A. Sanz-Medel, *TrAC Trends Anal. Chem.* **2006**, *26*, 958–967.
- [5] a) A. Salinas-Castillo, I. Sánchez-Barragán, J. M. Costa-Fernández, R. Pereiro, A. Ballesteros, J. M. González, A. Segura-Carretero, A. Fernández-Gutiérrez, A. Sanz-Medel, *Chem. Commun.* **2005**, 3224–3226; b) I. Sánchez-Barragán, J. M. Costa-Fernández, R. Pereiro, A. Sanz-Medel, ; A. Salinas, A. Segura, A. Fernández-Gutiérrez, A. Ballesteros, J. M. González, *Anal. Chem.* **2005**, *77*, 7005–7011; c) J. M. Traviesa-Alvarez, I. Sánchez-Barragán, J. M. Costa-Fernández, R. Pereiro, A. Sanz-Medel, *Analyst* **2007**, *132*, 218–223; d) T. Zhou, N. Wang, C. Li, H. Yuan, D. Xiao, *Anal. Chem.* **2010**, *82*, 1705–1711; e) Y. Li, X. Liu, H. Yuan, D. Xiao, *Biosens. Bioelectron.* **2009**, *24*, 3706–3710.
- [6] a) Y. He, H.-F. Wang, X.-P. Yan, *Anal. Chem.* **2008**, *80*, 3832–3837; b) H.-F. Wang, Y. He, T.-R. Ji, X.-P. Yan, *Anal. Chem.* **2009**, *81*, 1615–1621; c) Y. He, H.-F. Wang, X.-P. Yan, *Chem. Eur. J.* **2009**, *15*, 5436–5440; d) P. Wu, Y. He, H.-F. Wang, X.-P. Yan, *Anal. Chem.* **2010**, *82*, 1427–1433.
- [7] a) C. C. Huang, S. H. Chiu, Y. F. Huang, H. T. Chang, *Anal. Chem.* **2007**, *79*, 4798–4804; b) X. Y. Xu, Z. Zhao, L. D. Qin, W. W. , J. E. Levine, C. A. Mirkin, *Anal. Chem.* **2008**, *80*, 5616–5621; c) J. Wang, Y. X. Jiang, C. S. Zhou, X. H. Fang, *Anal. Chem.* **2005**, *77*, 3542–3546; d) C. C. Huang, H. T. Chang, *Anal. Chem.* **2006**, *78*, 8332–8338.
- [8] a) P. Janda, J. Weber, L. Dunsch, A. B. P. Lever, *Anal. Chem.* **1996**, *68*, 960–965; b) M. N. Zhang, K. Liu, L. Xiang, Y. Q. Lin, L. Su, L. Q. Mao, *Anal. Chem.* **2007**, *79*, 6559–6565; c) S. S. L. Castro, V. R. Balbo, P. J. S. Barbeira, N. R. Stradiotto, *Talanta* **2001**, *55*, 249–254.
- [9] a) A. Bossi, S. A. Piletsky, E. V. Piletska, P. G. Righetti, A. P. F. Turner, *Anal. Chem.* **2000**, *72*, 4296–4300; b) K. Güçlü, K. Sözgen, E. Tütem, M. Özyürek, R. Apak, *Talanta* **2005**, *65*, 1226–1232.
- [10] a) W. S. Kim, R. L. Dahlgren, L. L. Moroz, J. V. Sweedler, *Anal. Chem.* **2002**, *74*, 5614–5620; b) V. Gökmen, N. Kahraman, N. Demir, J. Acar, *J. Chromatogr. A* **2000**, *881*, 309–316.
- [11] S. Vermeir, B. M. Nicolai, P. Verboven, P. Van Gerwen, B. Baeten, L. Hofflack, V. Vulsteke, J. Lammertyn, *Anal. Chem.* **2007**, *79*, 6119–6127.
- [12] W. B. Chen, X. Wang, X. J. Tu, D. J. Pei, Y. Zhao, X. Q. Guo, *Small* **2008**, *4*, 759–764.
- [13] Y. J. Chen, X. P. Yan, *Small* **2009**, *5*, 2012–2018.
- [14] J. Q. Zhuang, X. D. Zhang, G. Wang, D. M. Li, W. S. Yang, T. J. Li, *J. Mater. Chem.* **2003**, *13*, 1853–1857.
- [15] R. Y. Tu, B. H. Liu, Z. Y. Wang, D. M. Gao, F. Wang, Q. L. Fang, Z. P. Zhang, *Anal. Chem.* **2008**, *80*, 3458–3465.
- [16] H. C. Warad, S. C. Ghosh, B. Hemtanon, C. Thanachayanont, J. Dutta, *Sci. Technol. Adv. Mater.* **2005**, *6*, 296–301.
- [17] a) J. F. Suyver, S. F. Wuister, J. J. Kelly, A. Meijerink, *Nano Lett.* **2001**, *1*, 429–433; b) H. Yang, S. Santra, P. H. Holloway, *J. Nanosci. Nanotechnol.* **2005**, *5*, 1364–1375.
- [18] E. Mohagheghpour, M. Rabiee, F. Moztarzadeh, M. Tahriri, M. Jafarbeglou, D. Bizari, H. Eslami, *Mater. Sci. Eng. C* **2009**, *29*, 1842–1848.
- [19] a) M. Otsuka, T. Kurata, N. Arakawa, *Agric. Biol. Chem.* **1986**, *50*, 531–533; b) M. Ohmori, M. Takagi, *Agric. Biol. Chem.* **1978**, *42*, 173–174.
- [20] X.-F. Wang, J.-J. Xu, H.-Y. Chen, *J. Phys. Chem. C* **2008**, *112*, 17581–17585.
- [21] R. N. Bhargava, D. Gallagher, X. Hong, A. Nurmikko, *Phys. Rev. Lett.* **1994**, *72*, 416–419.
- [22] I. Yu, T. Isobe, M. Senna, *J. Phys. Chem. Solids* **1996**, *57*, 373–379.

Received: April 24, 2010
Published online: September 23, 2010